IOSR Journal of Mechanical and Civil Engineering (IOSR-JMCE)
e-ISSN: 2278-1684,p-ISSN: 2320-334X, Volume 20, Issue 2 Ser. II (Mar. – Apr. 2023), PP 61-75
www.iosrjournals.org

Strain-Hardening Cementitious Composites Versus Normal Mortar for Shear Strengthening of Concrete Beams

Reda N. Behiry[1], Tamer M. El Korany[2]
[1](Assistant Professor, Structural Engineering Dept., Faculty of Engineering, Tanta University, Tanta, Egypt)
[2](Associate Professor, Structural Engineering Dept., Faculty of Engineering, Tanta University, Tanta, Egypt)

Abstract: *Strain-Hardening Cementitious Composites (SHCC) are distinct from normal mortar (NM) in that it has the ability to control crack width and exhibits ductile tensile strain-hardening behavior. The effectiveness of NM and SHCC as a strengthening jacket for concrete beams with shear deficiencies was assessed in the current study. Nine simply supported concrete beams are prepared; three of them were control specimens without web reinforcement in the studied region, whereas the others were either SHCC jackets or NM jackets. The key parameters comprised of the shear span-to-depth ratios (a/d = 1.50, 2.25, and 3.00), as well as SHCC or NM as the matrix of the strengthening jacket. The test results showed that the shear behavior of SHCC-strengthened beams is much superior to that of NM jackets. Particularly, the shear capacity, initial stiffness, and energy absorption capacity of SHCC-strengthened beams were found to be considerably higher than those of the comparable NM jackets by an average of 30%, 35%, and 47%, respectively. Moreover, the SHCC jackets were capable of providing a significant reduction in the developed major shear crack width. On average, the crack width of SHCC-strengthened beams was approximately 44% smaller than it was in the NM-strengthened beams. Finally, it can be advised to use SHCC jackets instead of NM jackets for shear strengthening of concrete beams due to the superior properties of SHCC material in comparison to traditional NM.*

Keyword*: Shear-deficient beams; Strengthening; Strain-hardening cementitious composites (SHCC); Normal mortar (NM); Jacketing; Cracking behaviour, Energy absorption*.

Date of Submission: 20-03-2023 Date of Acceptance: 04-04-2023

I. Introduction

Several existing reinforced concrete structures constructed in the 19th and 20th centuries are deficient in shear, mostly due to the implementation of insufficient codes. So, these structures need to be rebuilt or strengthened to keep them functional; otherwise, catastrophic failures might occur. As a practical response to several difficulties, including economic and environmental constraints, strengthening reinforced concrete structures has recently grown in popularity in the construction fields relative to new construction. Different strengthening systems, such as concrete jacketing, steel jacketing, and external pre-stressing, have been suggested to improve the shear performance capacity of reinforced concrete structures. The material utilized is one of the most essential aspects influencing the success of the strengthening system. The compatibility of the substrate and the strengthening material is an important consideration in the selection of the strengthening material.

The use of externally bonded fiber-reinforced polymers (EB-FRP) in the shear strengthening of reinforced concrete beams has become increasingly common over the past two decades. However, as was mentioned in previous studies [1-10], the EB-FRP strengthening system has a few limitations that are primarily related to the use of epoxy resins. These limitations include poor performance at high temperatures and difficulties in application on wet surfaces. On contrast, jacketing is a widely used method for the retrofitting of reinforced concrete beams. This is primarily because, in addition to its capability of effectively improving the mechanical performance of structural members, it also possesses several other advantages over externally bonded fiber-reinforced polymers (EB-FRP) and externally bonded steel plates. These advantages include a simple construction technique, high durability, and adequate fire and corrosion resistance [11-16].

Currently, strain-hardening cementitious composites (SHCC), also called engineered cementitious composites (ECC), has been shown to be a good material for repairing and strengthening concrete structures in general. This is due to the SHCC's obvious benefits, which include high tensile strain capacity accompanied by the formation of fine multiple cracks, which is an important main criterion of a durable material in order to eliminate premature failures [17-21]. These benefits motivate scientists to investigate whether SHCC is practical at the structural level [22-28].

The shear transformation that occurs between the strengthening jacket and the substrate concrete is considered to be an essential aspect in the practice of external shear strengthening. Researchers [29-32] searched at how SHCC bonds to concrete and how concrete bonds to concrete, and they concluded that SHCC bonds to concrete were superior in comparison with concrete bonds to concrete. Regarding strengthening applications in literature, the shear behavior of SHCC-strengthened reinforced concrete beams was explored by Kim et al. [33], Wang et al. [34], and Hassan et al. [35]. The results of their experimental study demonstrated that using SHCC as an external strengthening layer was able to increase the ductility and shear capacity of the tested specimens. In addition, it was concluded that the SHCC layer was successful in improving the cracking behavior. Studies were carried out by Baghi et al. [36], Afefy et al. [37], Baraghith et al. [38,39], and Khalil et al. [40] to assess whether or not the use of precast SHCC plates as an external strengthening method for deficient concrete beams was effective. They demonstrated that the utilization of precast SHCC plates was a smart strategy for enhancing the shear capacity and arresting the crack propagation.

According to the information that was provided in the preceding section, the majority of the earlier research was carried out to evaluate the structural performance of SHCC materials when used to strengthen RC beams with a shear span-to-depth ratio that was close to 3.00. So, the purpose of this paper is to investigate the shear capacity, stiffness, energy absorption capacity, and failure mechanisms of reinforced concrete beams that have been strengthened with normal mortar (NM) and strain-hardening cementitious composites (SHCC) jackets. Moreover, the shear behavior of strengthened reinforced concrete beams using NM and SHCC jackets with varied shear span-to-depth ratios (1.50, 2.25, and 3.00) were experimentally studied.

II. Experimental Program

2.1 Materials

Every test specimen was simultaneously cast in plywood formworks and cured with wet burlap. Ready-mixed concrete was utilized for the construction of the concrete substrate. The coarse aggregates had a weight of 919 kg/m^3 and consisted of crushed limestone with a maximum nominal size of 20mm. Moreover, the mix contained 843 kg/m^3 of natural sand, 294 kg/m^3 of Ordinary Portland Cement (OPC-type I), and 185 kg/m^3 of water. Casting of three standard cylinders, each measuring 300 millimeters in height and 150 millimeters in diameter, took place on the same day as the specimens. After a total of 28 days, the compressive strength of the substrate concrete, on average, was 25.2 MPa according to ASTM standard [40]. Mixing the strain-hardening cementitious composites (SHCC) required the use of ingredients that were already well-combined, such as quartz sand, Ordinary Portland Cement (OPC-type I 52.5R), and fine silica fume with an average diameter of 0.2 millimeters. For the purpose of ensuring that the SHCC mixture is easy to work with, the Sika viscocrete superplasticizer (SP) was used in conjunction with a water-to-binder ratio that was kept relatively low at 0.20. As internal reinforcement, the Sika Company's 12 mm diameter by 0.012 mm wide polypropylene (PP) discrete fiber was used. On the other hand, without the inclusion of any additional additives, the normal mortar (NM) mixture was made up of fine aggregates (sand), Ordinary Portland Cement (OPC-type I 52.5R), and a water/cement ratio of 0.50. Table 1 lists the materials' design proportions for substrate concrete, normal mortar (NM), and strain-hardening cementitious composites (SHCC).

Table 1 Mix proportions of substrate concrete, normal mortar, and SHCC materials (kg/m^3).

Mix	W/B*	Cement	Sand	Coarse aggregates	Water	Silica fume	Super-plasticizer	PP Fiber (12 mm)
Substrate concrete	0.63	294	843	919	185	---	---	---
Normal mortar	0.50	294	1762	---	147	---	---	---
SHCC	0.20	1243	149	---	292	223	14.9	14.6

* W/B is the water/ binder ratio, B = cement + silica fume.

In order to determine the compressive strengths of SHCC and NM in accordance with the requirements of ASTM standard [41], three standard cylinders, each measuring 100 millimeters in diameter and 200 millimeters in height, were cast during the production processes of SHCC and NM. In addition, the uniaxial tensile testing method developed by Elnagar et al. [42] (see Fig. 1) was used to obtain the tensile stress-strain relationship of the NM and SHCC materials using six prisms, one of which was 50 millimeters in thickness, 150 millimeters in width, and 500 millimeters in height. The average values of NM's compressive strength and tensile strength were determined to be 28.0 and 3.44 MPa, whereas the corresponding values for SHCC materials were 80.0 and 7.23 MPa. Additionally, in order to quantify the cracking behavior of both NM and SHCC materials, Fig. 2 depicts the crack mapping that was performed following complete tensile failure for both types of materials. It can be clearly

concluded that the cracks appeared in a finely dispersed pattern across the SHCC prism and that the number of cracks was significantly higher in the SHCC prism than it was in the NM prism.

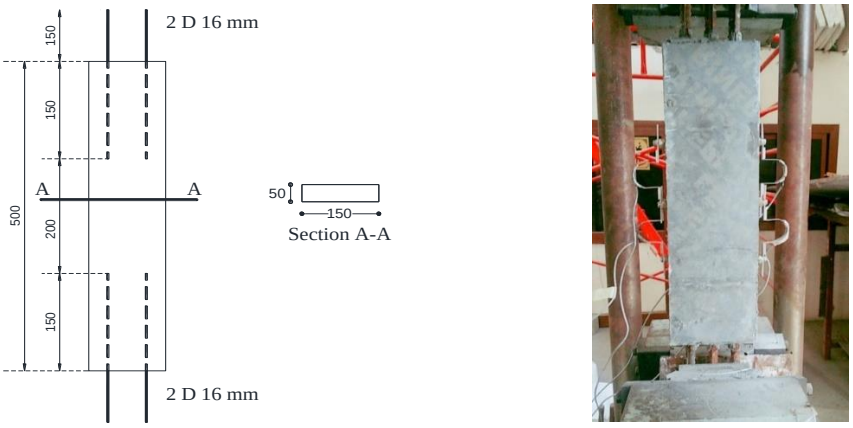

(a) Dimension of test specimens. (b) Test setup and instrumentation.

Fig. 1. Uniaxial tensile testing of prism-shaped NM and SHCC specimens (All dimensions in mm).

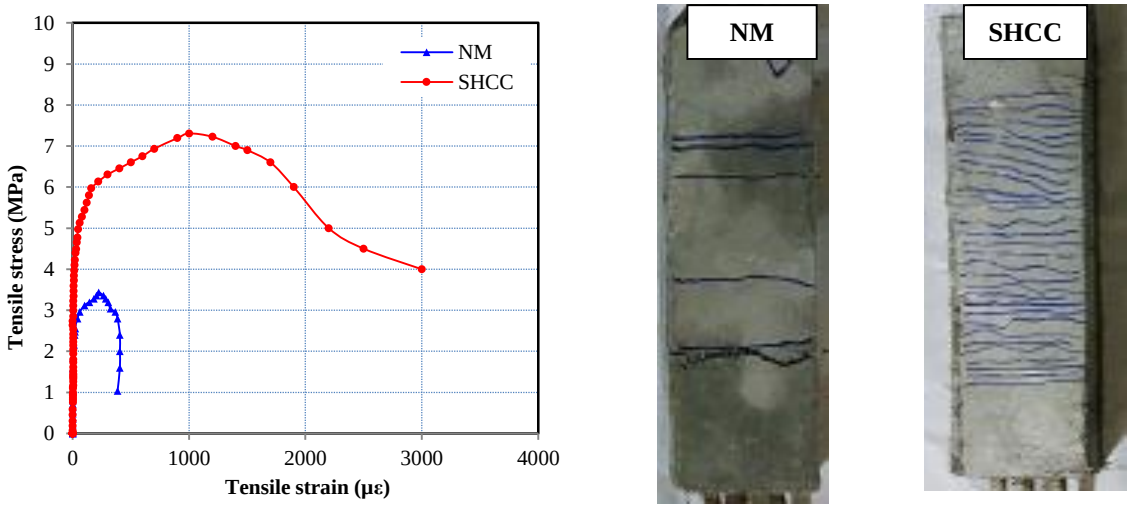

(a) Tensile stress-strain curves. (b) Cracks' distribution.

Fig. 2. Tensile behaviour responses of NM versus SHCC.

Within the framework of the experimental program, smooth bars with diameters of 6 and 8 millimeters were used as shear reinforcement, while ribbed bars with diameters of 16 and 22 millimeters were used for flexural reinforcement. Uniaxial tensile tests on reinforcing bars were carried out in accordance with the requirements of the ASTM standard [43] to obtain the stress-strain characteristics of the reinforcements. The yield strengths of the bars having a diameter of 6, 8, 16, and 22 mm were 285, 248, 452, and 431 MPa, respectively, whereas their ultimate strengths were 399, 382, 619, and 605 MPa, respectively. Table 2 summarizes the results of the tested bars, and it can be seen that the ultimate strain was somewhere in the range of 19000-24000 $\mu\varepsilon$, whereas the yielding strain was anywhere from 1240 to 2260 $\mu\varepsilon$.

Table 2 Properties of the steel reinforcement using uniaxial tensile test.

Diameter Φ (mm)	Yielding strength f_y (MPa)	Ultimate strength f_u (MPa)	Yielding strain ε_y (με)	Ultimate strain ε_u (με)
6	285	399	1425	24000
8	248	382	1240	22000
16	452	619	2260	21000
22	431	605	2155	19000

2.2 Specimens and experimental parameters

The tests were conducted on nine full-scale, rectangular reinforced concrete beams that were simply supported. The tested beams' overall length was 2700 millimeters, while their effective length was 2400 millimeters. The cross-sectional dimensions of the concrete were 150 millimeters in width and 350 millimeters in total height; the effective depth (d) equals 300 millimeters. The shear span (a) ranged from 450 to 900 millimeters, resulting in three distinct shear span-to-depth ratios, denoted by the notation a/d = 1.50, 2.25, and 3.00, respectively. To make sure shear failure occurred before flexural failure, three lower longitudinal steel bars with a diameter of 22 millimeters were used as tensile reinforcement. In addition, two upper longitudinal steel bars with a diameter of 16 millimeters were used as compressive reinforcements. Moreover, each of the tested specimens was designed with a shear deficiency in one of the two shear spans. As a result, the left shear span (the studied zone) was devoid of stirrups, while the other shear span had stirrups with an 8 mm diameter and a 75 mm spacing as recommended by ACI 318-19 [44]. The geometry and arrangement of the internal steel rebars for the tested specimens are shown in Fig. 3.

To enhance the shear behavior of reinforced concrete beams, a 20 mm-thick jacket of either normal mortar (NM) or strain-hardening cementitious composites (SHCC) was applied to the sides of shear-deficient zone. The key parameters in this research are (a) the type of material used in the strengthening jacket (NM or SHCC) and (b) the shear span-to-depth ratio (a/d). As shown in Table 3, the un-strengthened specimens were defected in the shear zone with shear span-to-depth ratios equal to 1.50, 2.25, and 3.00. While the remaining six specimens were strengthened using normal mortar or SHCC jackets. The strengthened jacket with a thickness of 20 mm is reinforced with vertical shear reinforcement of 6 mm diameter at a spacing of 150 mm (see Fig. 4). The notation of the specimens is XY-Z, where "X" denotes a beam, "Y" denotes a control or strengthened specimen ("C" for control specimens without any strengthening, "N" for strengthened specimens using normal mortar jacket, and "S" for strengthened specimens using SHCC jacket), and "Z" denotes the value of the shear span-to-depth ratio (1.50, 2.25, or 3.00).

Table 3 Details of the test matrix.

Specimen	Characteristics	Shear span (a)	a/d	Mortar type
BC-1.50	Control specimen with shear span to depth ratio of 1.50	450	1.50	--
BN-1.50	Strengthened specimen using normal mortar jacket with shear span to depth ratio of 1.50	450	1.50	Normal mortar
BS-1.50	Strengthened specimen using SHCC jacket with shear span to depth ratio of 1.50	450	1.50	SHCC
BC-2.25	Control specimen with shear span to depth ratio of 2.25	675	2.25	--
BN-2.25	Strengthened specimen using normal mortar jacket with shear span to depth ratio of 2.25	675	2.25	Normal mortar
BS-2.25	Strengthened specimen using SHCC jacket with shear span to depth ratio of 2.25	675	2.25	SHCC
BC-3.00	Control specimen with shear span to depth ratio of 3.00	900	3.00	--
BN-3.00	Strengthened specimen using normal mortar jacket with shear span to depth ratio of 3.00	900	3.00	Normal mortar
BS-3.00	Strengthened specimen using SHCC jacket with shear span to depth ratio of 3.00	900	3.00	SHCC

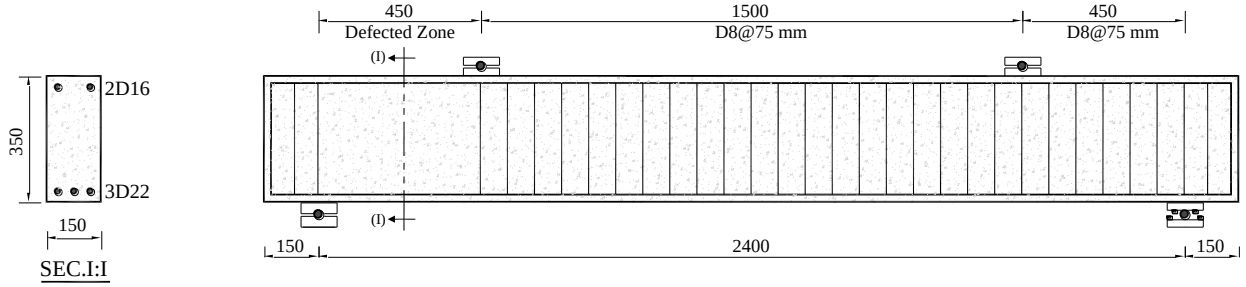

(a) Specimens with shear span to depth ratio (a/d = 1.50)

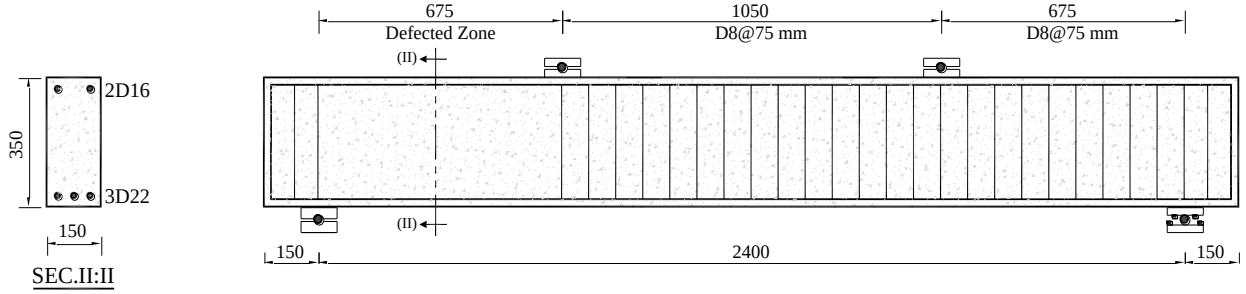

(b) Specimens with shear span to depth ratio (a/d = 2.25)

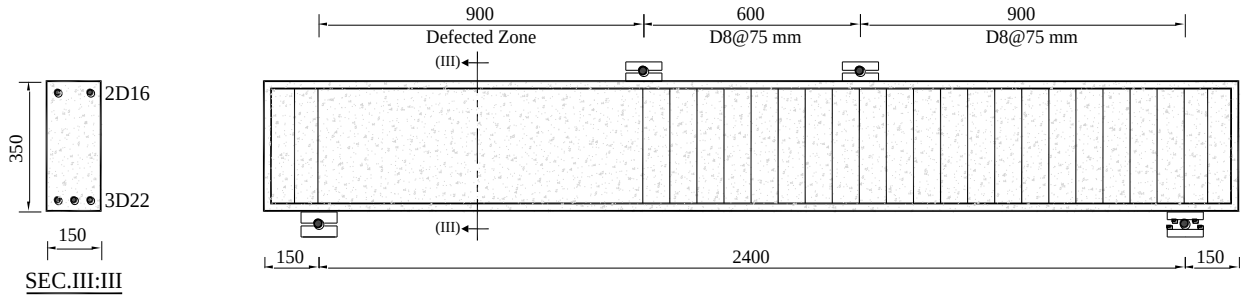

(c) Specimens with shear span to depth ratio (a/d = 3.00)

Fig. 3. Geometry and internal steel reinforcements of the tested specimens (All dimensions in mm).

2.3 Strengthening procedure

Compatibility between the substrate concrete and the jacket surfaces is a key aspect of the success of the strengthening techniques. So, one of the most typical failure scenarios is the separation of the strengthening jacket from the substrate concrete; in other words, this failure is known as debonding failure. In order to prevent this failure, as shown in Fig. 5(a), the surface of the substrate concrete was roughened with a chisel to remove the cement slurry around coarse aggregates. Thereafter, an air blower was used to clean the concrete surface. Prior to casting the strengthening jacket, Kemapoxy 104 epoxy resin, locally produced by CMB Company, was first prepared and applied on the surface of substrate concrete to improve the bond mechanism between the strengthening jacket and substrate concrete (Fig. 5(b)). Then, the jacket reinforcement was fixed as shown in Fig. 5(c). In the final step, the jacket was cast with a thickness of 20 mm using a wooden shuttering as shown in Fig. 5(d). Before being tested, the NM- and SHCC-strengthened concrete beams were cured for 28 days with wet burlap at room temperature.

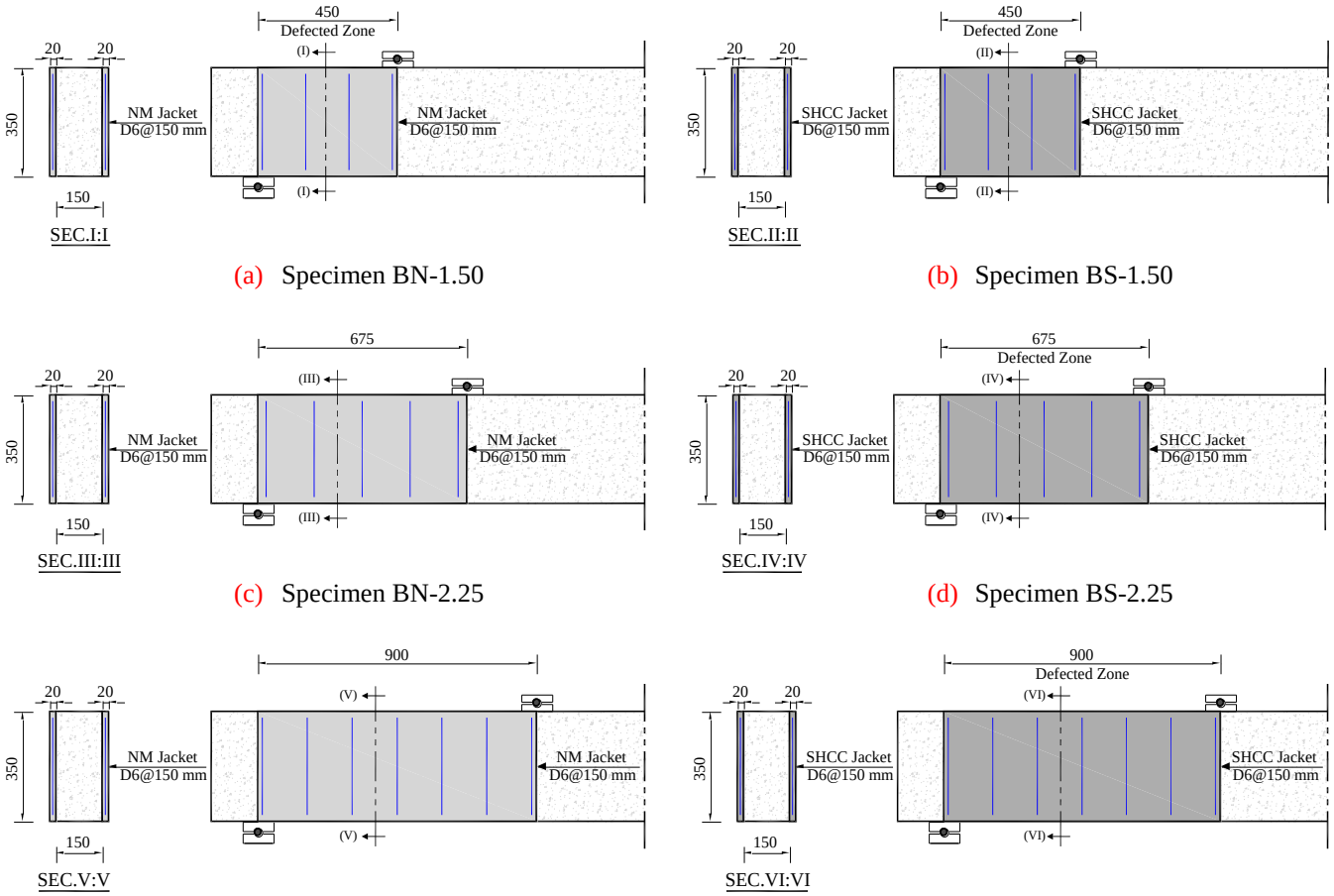

(a) Specimen BN-1.50 (b) Specimen BS-1.50

(c) Specimen BN-2.25 (d) Specimen BS-2.25

(e) Specimen BN-3.00 (f) Specimen BS-3.00

Fig. 4. Scheme of the strengthened specimens (All dimensions in mm).

(a) Removal of concrete cover **(b)** Applying the epoxy resin prior casting the jacket

(c) Fixation of the jacket reinforcement **(d)** Final jacket after casting

Fig. 5. Strengthening application process.

2.4 Loading and test scheme

Every specimen was tested through monotonic loading using a four-point loading methodology, which is depicted in Fig. 6. The tested specimen rested on two supports, the right one being a hinge and the left one being a roller. The load was gradually applied using a load cell that has a capacity of 850 kN. Four linear variable

differential transformers (LVDTs) were utilized to quantify vertical deflections at different loading stages. A pair of LVDTs were installed under the span's midpoint and loading point, and a pair more were installed above the supporting points to get the net deflection of the tested specimen. Moreover, two 45-degree LVDTs (Rosette) [45] were installed in the center of the shear span to record the diagonal crack width as well as the associated shear stresses. Electrical strain gauges (6.0 mm-long) were attached to the tensile reinforcement in the mid-span zone and the jacket reinforcement to measure the axial strain that had been generated in the bars. Furthermore, an electrical Pi-gauge was used to estimate the maximum compressive strain in the concrete at the mid-flexural region. During testing of each specimen, a data collecting device recorded all experimental measurements, including loads, deflections, and strains.

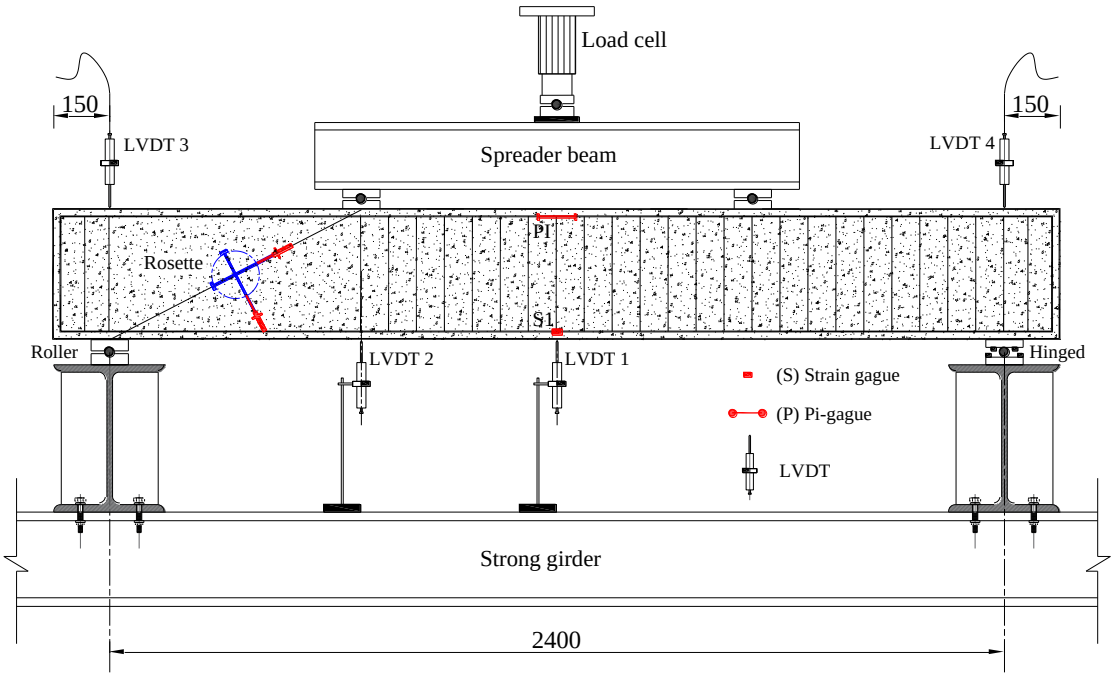

Fig. 6. Test setup and instrumentation (All dimensions in mm).

III. Test results and discussion

3.1 Failure patterns

The failure modes of the test specimens are shown in Fig. 7. In general, the propagation of diagonal shear cracks within the investigated region resulted in shear failure patterns in both the control (un-strengthened) and strengthened specimens. At the beginning of loading, flexural cracks first appeared in all of the specimens in the constant moment zone, which is the middle of the span. Then, the main diagonal shear crack started at the mid-height of the specimen and extended along the diagonal line between the loading and support points. By increasing the load up to failure, secondary diagonal cracks appeared, and the width of these cracks gradually grew wider.

Concerning to a shear span-to-depth ratio (a/d) of 1.5, inclined cracks propagated rapidly from the applied load in the compression zone towards the flexural reinforcement. Near to failure, no new inclined cracks were developed, and the established cracks stabilized without further propagation, although their widths grew. The main reason that contributed to the final failure of the specimen was the rapid growth of the critical diagonal crack into the compression zone close to the load point. This was induced by a uniaxial stress condition at the crack's tip: compression parallel to the crack. Conventionally, this type of failure is known as a shear compression failure. On the other hand, for the specimens with a/d values of 2.25 and 3.50, the critical failure stress was diagonal tension perpendicular to the crack. This mode of failure is conventionally called shear tension failure.

Regarding the type of jacket's material, the failure mode of the strengthened specimens with normal mortar jackets (BN-1.50, BN-2.25, and BN-3.00) was sudden and brittle, with a single large crack. On the other hand, the mode of failure for all strengthened specimens with SHCC jackets was more ductile and accompanied by multiple narrower diagonal cracks. It was evidently attributable to the bridging effect of the discontinuous polypropylene fibers present inside SHCC components. It's worth noting the shear reinforcement contained inside the strengthening jacket reached to the yielding strain, and there was no evidence of separation between the substrate concrete and the jacket.

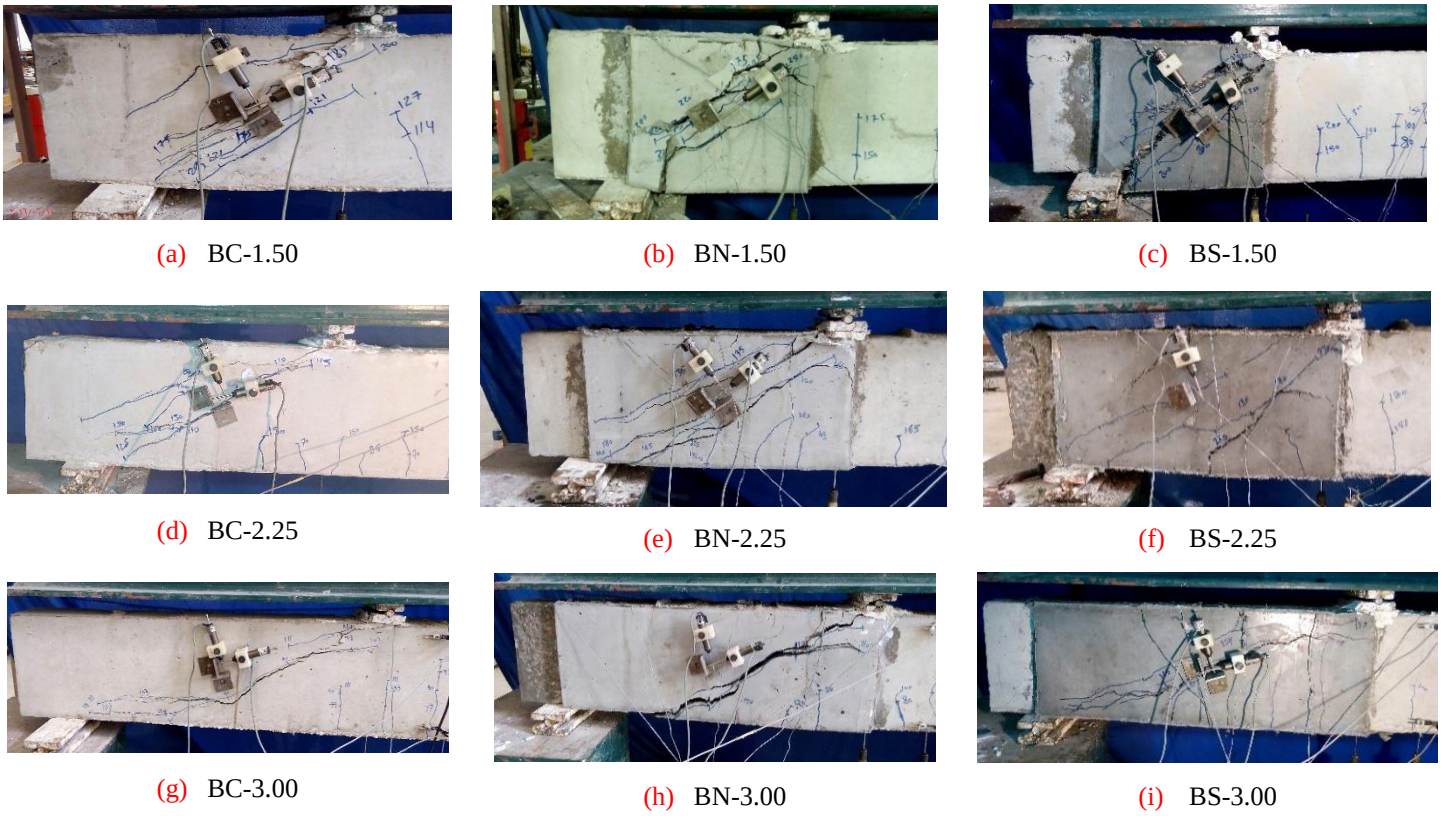

(a) BC-1.50 (b) BN-1.50 (c) BS-1.50

(d) BC-2.25 (e) BN-2.25 (f) BS-2.25

(g) BC-3.00 (h) BN-3.00 (i) BS-3.00

Fig. 7. Failure mode for all tested specimens.

3.2 Cracking and ultimate loads

Table 4 shows a summary of the results of the experiments. It shows the diagonal cracking load (P_{cr}), the ultimate load (P_u), and the gain capacity due to the proposed strengthening technique. Concerning the results of the cracking loads, the increases in cracking capacity for strengthened specimens with SHCC jackets are significant compared to NM jackets (23.4% average). These results confirm that the SHCC jacket is more effective than the NM one due to the superior tensile properties of the SHCC material compared to the normal mortar (NM), as concluded before from Fig. 2(a).

To talk about how the efficiency of the proposed SHCC strengthening jacket compares to the NM jacket, the gains in ultimate loads for the strengthened specimens are calculated with respect to their counterpart un-strengthened specimens and listed in Table 4. It can be concluded that the overall respective gains in ultimate load capacity for SHCC-strengthened specimens were a minimum of 57.7% for a/d = 3.00 and a maximum of 85.7 % for a/d = 1.50 relative to the un-strengthened specimens. Also, using SHCC jackets as a strengthening system instead of NM jackets generally had a significant enhancement in the ultimate load of the strengthened specimens. In particular, the ultimate shear capacities of SHCC-strengthened specimens BS-1.50, BS-2.25, and BS-3.00 represented a 30%, 28%, and 32% increase over the NM-strengthened specimens BN-1.50, BN-2.25, and BN-3.00, respectively.

Table 4 Experimental results.

Specimen	Loads (kN)			Deflections (mm)		Stiffness (kN/mm)		Energy absorption (kN.mm)		Crack width (mm)		Maximum strain (με)		
	P_{cr}	P_u	Capacity* gain %	Δ_{cr}	Δ_{max}	k_i	Gain* %	E_u	Gain* %	w_{cr}	Reduction* %	ε_s	ε_{sw}	ε_c
BC-1.50	178.3	214.3	--	3.55	4.58	44.7	--	247	--	0.74	--	1068	1235	1714
BN-1.50	259.8	306.1	42.8	4.82	6.57	56.0	25.3	543	119.8	0.62	16.2	1473	1309	2277
BS-1.50	328.2	397.9	85.7	4.27	7.19	79.2	77.2	761	208.0	0.39	47.3	1645	1872	2519
BC-2.25	118.4	151.0	--	3.89	5.76	33.0	--	234	--	1.05	--	1167	2135	1984
BN-2.25	157.2	201.4	33.3	4.54	6.34	36.8	11.5	348	48.7	0.85	19.0	1419	2406	2195
BS-2.25	196.1	258.5	71.1	3.95	8.07	52.2	58.2	461	97.0	0.51	51.4	1598	2765	2456
BC-3.00	87.5	111.7	--	3.52	5.67	24.9	--	180	--	1.42	--	1132	2605	1863
BN-3.00	99.7	133.8	19.8	3.31	6.15	30.1	20.9	246	36.7	1.10	22.5	1346	2816	2044
BS-3.00	118.9	176.2	57.7	3.28	8.63	36.3	45.8	411	128.3	0.50	65.8	1506	3125	2401

** Calculated relative to their counterpart un-strengthened specimens*

P_{cr} = first shear cracking load; P_u = ultimate load; Δ_{cr} = deflection corresponding to the first shear cracking load; Δ_{max} =deflection corresponding to the 0.85 P_u after the peak point; k_i = initial stiffness; E_u = energy absorption; w_{cr} = crack width corresponding to the 0.85 P_u before the peak point ; ε_s is the maximum tensile strain of main reinforcement at mid-span section; ε_{sw} is the maximum developed tensile strain in the reinforcement embedded inside the jacket; ε_c is the maximum compressive strain in concrete at mid span-section.

3.3 Load-deflection behaviors

The net load-deflection relationships of the control and strengthened specimens are shown in Figs. 8(a) through 8(c). In general, both the NM and SHCC strengthening jackets are better than the control specimens in how they respond to deflection, how stiff they are at first, and how much energy they can absorb. Up until the diagonal cracking load, the relationship between the applied load and the net deflection is almost linear for all tested specimens, with or without strengthening. As the load grows up until failure, deflection tends to rise quickly and move away from a straight line. It's important to note that the post-peak behavior of the strengthened specimens is different from that of the control specimen based on the experimental parameters.

Each specimen's displacement capacity (Δ_{max}) was determined as the point at which a 15% drop in the maximum sustained load was recorded; this degree of displacement would result in significant damage to the specimen [46]. The corresponding displacement capacity values for each test specimen are listed in Table 4. It can be observed that the displacement capacities (Δ_{max}) of the strengthened specimens using NM and SHCC jackets are generally higher than those of the control specimens, with an average value of 21% and 50%, respectively. Comparing the results obtained for specimens strengthened with SHCC jacket and NM jacket indicates that specimens with SHCC jacket showed higher displacement capacity (Δ_{max}) compared to those with NM jacket by about 9%, 27%, and 40% for a/d ratios of 1.50, 2.25, and 3.00, respectively. This is due to the crack-arresting effect offered by SHCC materials.

3.4 Initial stiffness

The slope of the load-deflection curve before it cracked was used to figure out the initial stiffness (k_i) [47]. Table 4 demonstrates that the initial stiffness of all the strengthened specimens was higher than that of the un-strengthened specimens with respect to the influence of the shear span-to-depth ratio. The initial stiffness of the strengthened specimens with NM jackets was 25.3%, 11.5%, and 20.9% higher than that of the control specimens with a/d = 1.50, 2.25, and 3.00. While these values were 77.2%, 58.2%, and 45.8% for strengthened specimens with SHCC jackets, these results clarify that the initial stiffness was noticeably impacted by using SHCC as opposed to NM. So, since SHCC material has superior properties than traditional NM, it may be better to use SHCC jackets instead of NM jackets to strengthen shear- deficient concrete beams.

3.5 Energy absorption

Energy absorption (E_u) is one of the ductility indicators used to investigate how well strengthened specimens can bear larger non-elastic deformations before failure, which is defined as the area under the load-deflection curve from the initial point to the peak point [48]. In this manner, the un-strengthened specimen BC-3.00 with an a/d ratio of 3.00 had the energy absorption value that was reported as having the lowest value (180 kN.mm). Whereas, using NM and SHCC jackets to strengthen this control specimen (BC-3.00) showed an increase in energy absorption of about 36.7% and 128.3%, respectively. Additionally, using the SHCC jacket instead of the NM jacket resulted in a significant increase in energy absorption. Compared to the strengthened specimens

BN-1.5, BN-2.25, and BN-3.00, the strengthened specimens BS-1.5, BS-2.25, and BS-3.00 were able to absorb 1.40, 1.32, and 1.67 times more energy, respectively. Overall, it was evident, based on the listed values in Table 4 of the gain in energy absorption, that utilizing the SHCC jacket as a strengthening system resulted in a superior improvement in the ductility behavior when compared to the un-strengthened specimens.

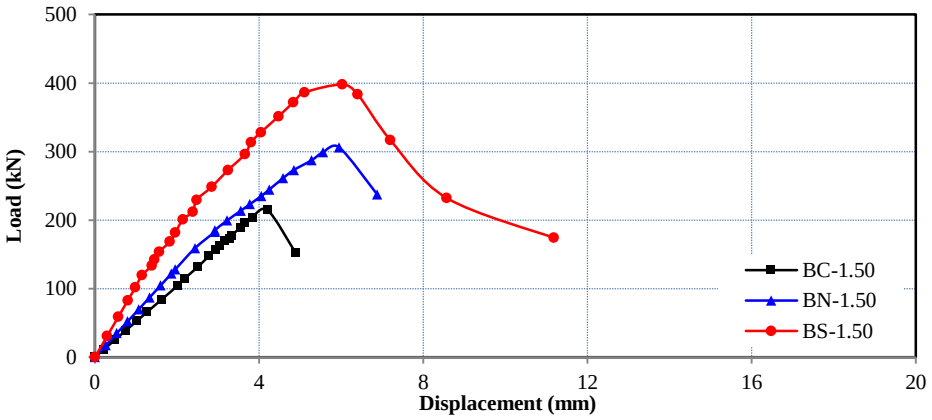

(a) Specimens with a/d=1.50

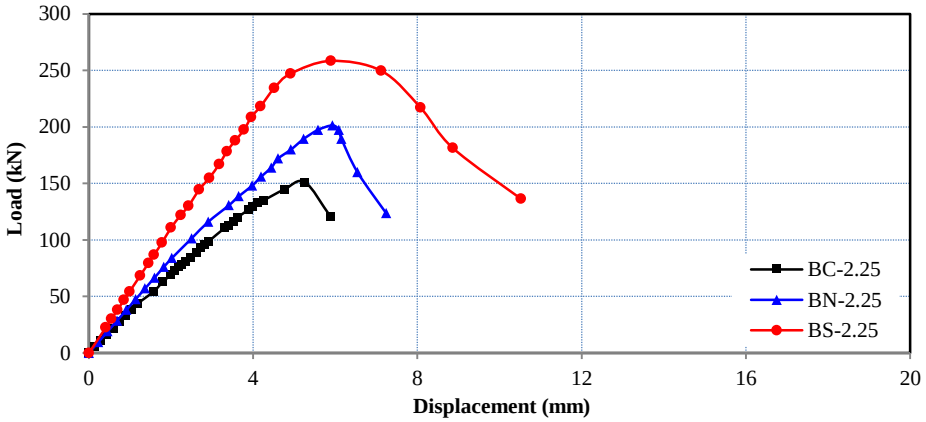

(b) Specimens with a/d=2.25

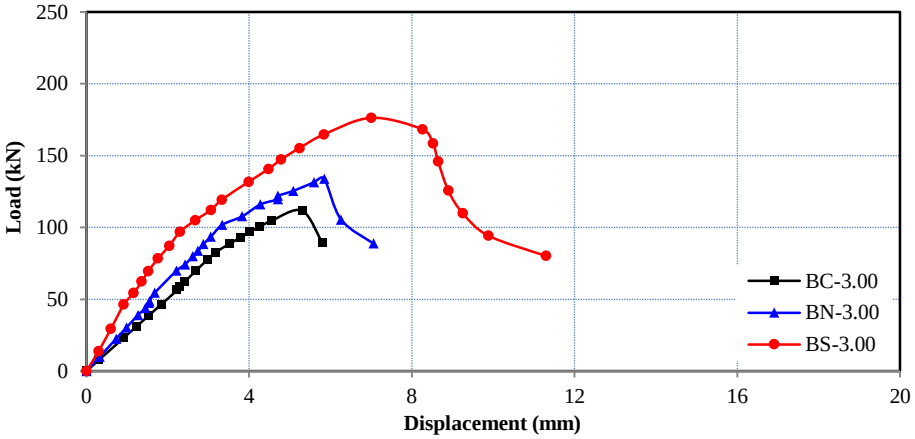

(c) Specimens with a/d=3.00

Fig. 8. Load-deflection responses.

3.6 Load-crack width behavior

The shear load-crack width curves for each of the specimens that were tested are depicted in Fig. 9. In terms of crack width reduction, SHCC-strengthened specimens were more effective than control specimens and strengthened specimens with NM jackets across all loading levels. Owing to the phenomenon of strain-hardening and the action of fiber-bridging, the SHCC inhibited crack propagation and reduced crack width. For instance, the crack width was narrow for SHCC-strengthened specimen BS-1.50 (0.39 mm) than that of control specimen BC-

1.50 (0.74 mm) at the same load level ($0.85P_u$). Furthermore, regarding the type of strengthening material (NM or SHCC), the shear crack widths obtained for specimens BN-1.50 (0.62 mm), BN-2.25 (0.85 mm), and BN-3.00 (1.10 mm) were all wider than those obtained for specimens BS-1.50 (0.39 mm), BS-2.25 (0.51 mm), and BS-3.00 (0.50 mm), respectively. According to reduction percentage values of crack width listed in Table 4, it was evident that the SHCC jacket strengthening method that had been used had kept crack widths under control up to the maximum load. This is because the SHCC materials' crack-arresting properties modified how cracks propagated and enhanced the serviceability of the strengthened specimens.

3.7 Strains

As depicted in Fig. 6, strain gauges were used to measure the maximum compressive strain of concrete, the tensile strain of flexural reinforcement, and the tensile strain of shear reinforcement, which was added inside the NM or SHCC jackets. For the reader's information, if an electric strain gauge showed erratic behavior that showed the reinforcement was coming loose before the specimen broke, the data points were taken away.

3.7.1 Compressive and tensile flexural strains

In Table 4, you can see the results of the tests on the maximum compressive strain (ε_c) of all tested specimens. The maximum value was observed for BS-1.50 ($\varepsilon_c = 2519\ \mu\varepsilon$), which did not reach the ultimate compressive strain in flexure ($\varepsilon_{cu} = 3000\ \mu\varepsilon$) according to ACI 318-19 [44]. This guaranteed that the failure mechanisms of these specimens were governed by shear rather than flexural failure. Furthermore, the tensile strains of flexural reinforcement (see Table 4) demonstrate the super-effectiveness of the suggested SHCC strengthening system. In other words, the maximum tensile strains of flexural reinforcement measured at failure for the strengthened specimens with SHCC jacket were almost more than 1.3 times those for the un-strengthened specimens. This indicates that the SHCC strengthening system played a superior role in delaying the failure of the non-ductile shear by letting the flexural steel move one step closer to the yield region.

3.7.2 Jacket reinforcement strains

The load-strain relationship for the jacket reinforcement of all strengthened specimens exhibited a bi-linear trend, as shown in Fig. 10. A straight line starting at the origin point and continuing along the vertical axis until the diagonal shear crack appears represents the first stage of the load-strain relationship. This means that the jacket reinforcement didn't help the shear strength of the strengthened specimens until the first shear crack appeared. Subsequent to the cracks' spread, the second stage was started by a sudden increase in the strains of jacket reinforcement. Finally, the relationship prolonged up to the yielding strain of hanger stirrups ($\varepsilon_y = 1200\ \mu\varepsilon$) and continued to increase up to failure load. As a brief note, the values of the jacket reinforcement strains at failure (ε_{sw}) for the strengthened specimens with SHCC jacket were in the range of 1872-3125 με; however, these values were in the range of 1309-2816 με for the strengthened specimen with NM jacket, as shown in Table 4. In other words, this result confirms that the SHCC jacket is able to increase the shear capacity and grant enhancements in the ductility performance of strengthened specimens compared to the NM jacket.

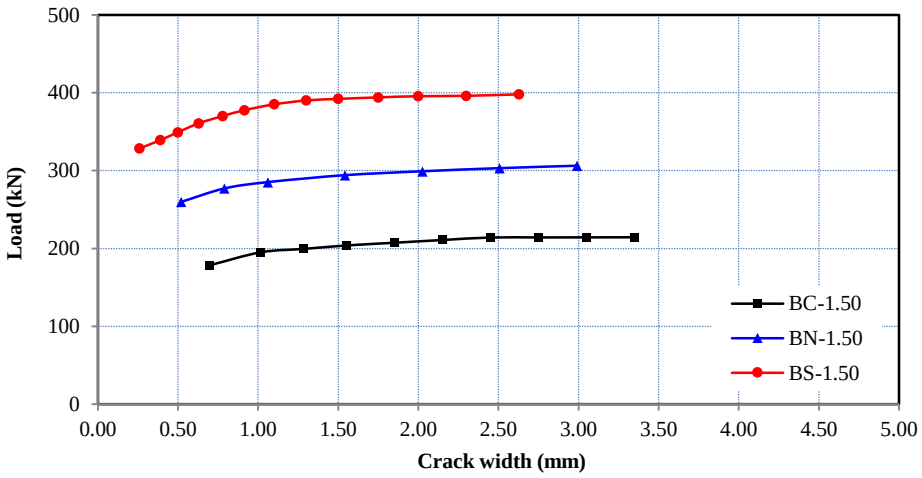

(a) Specimens with a/d=1.50

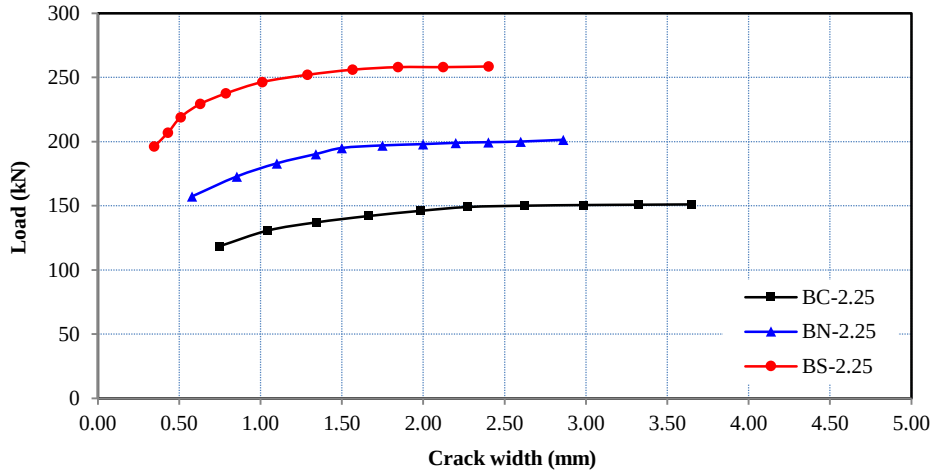

(b) Specimens with a/d=2.25

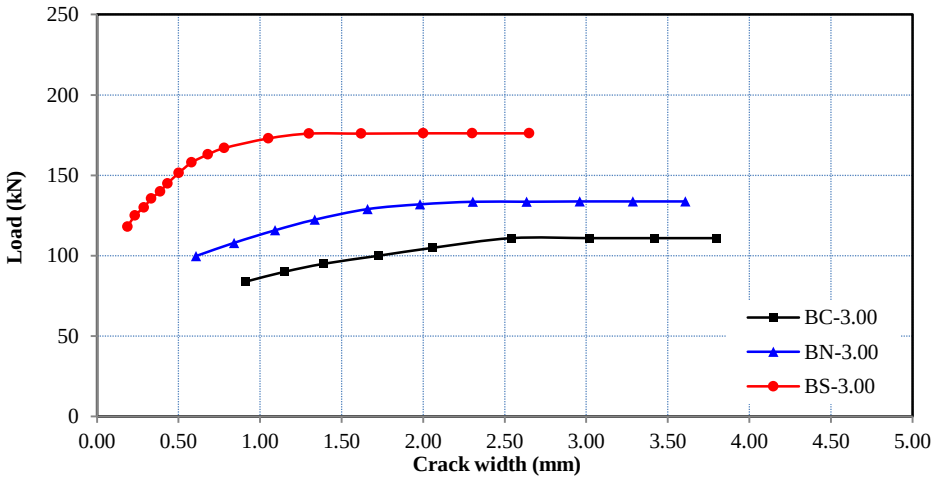

(c) Specimens with a/d=3.00

Fig. 9. Load-crack width behaviors.

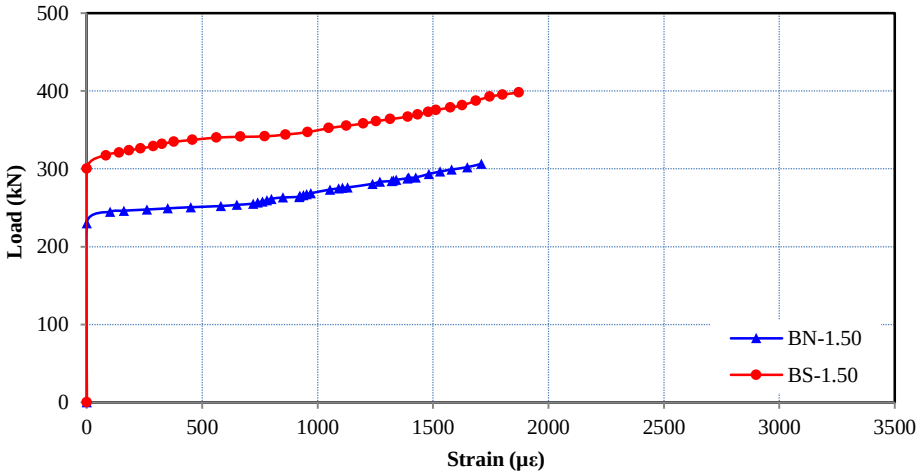

(a) Specimens with a/d=1.50

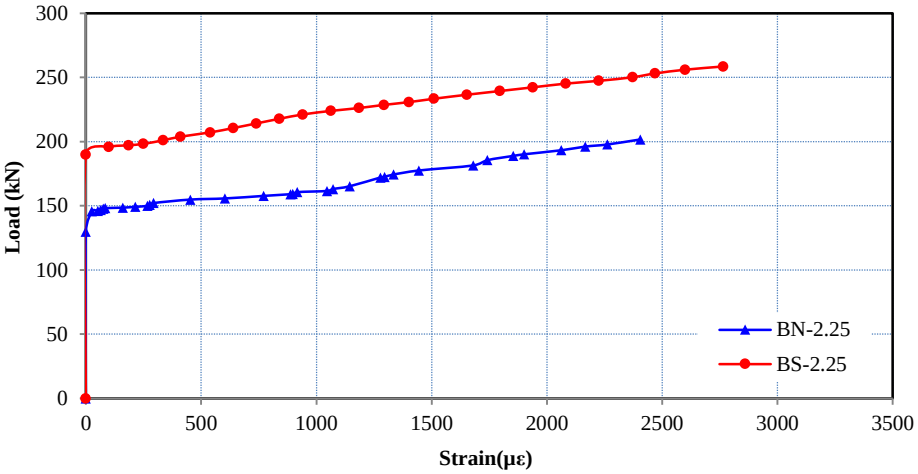

(b) Specimens with a/d=2.25

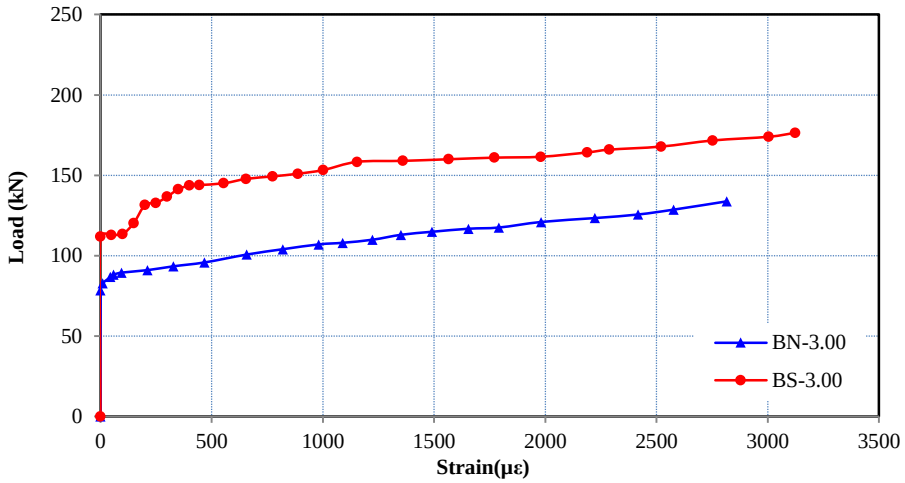

(c) Specimens with a/d=3.00

Fig. 10. Load-jacket reinforcement strain behaviors.

IV. Summary and Conclusion

Four-point bending tests were conducted to investigate the shear behavior of deficient concrete beams that were either strengthened with normal mortar (NM) or strain-hardening cementitious composites (SHCC) jackets. Using the present study's discussions as a guide, the following conclusions were drawn:

- In all ratios of shear span-to-depth (a/d), the ultimate load-carrying capacities of the SHCC-strengthened specimens were found to be higher than those of the corresponding NM jackets. In particular, SHCC-strengthened specimens BS-1.50, BS-2.25, and BS-3.00 had 30%, 28%, and 32% higher ultimate shear capacities than NM-strengthened specimens BN-1.50, BN-2.25, and BN-3.00, respectively.
- The load-carrying capabilities of the strengthened specimens decreased as the shear span-to-depth ratio increased, as predicted. The load-carrying capacity of the strengthened specimens with NM jackets decreased further when the a/d ratio was increased from 2.25 to 3.00.
- It concluded that the choice of material for strengthening has a significant effect on the initial stiffness. For all three a/d ratios, the initial stiffness of the NM jackets was found to be lower than that of the SHCC jackets by an average of 38%.
- At all a/d ratios, the ability of strengthened specimens with SHCC jackets to absorb energy was much greater than that of NM. This increment was significantly more pronounced in the strengthened specimens with a/d = 3.00.
- Compared to the NM jacketed specimens, the SHCC jacketed specimens were better at cracking in terms of load crack width response and shear-cracking load. For all strengthened specimens with SHCC jackets, at the same a/d ratio, the measured crack width was almost 40% less than that measured for strengthened specimens with NM jackets.

References

[1]. Triantafillou TC. Shear strengthening of reinforced concrete beams using epoxy-bonded FRP composites. ACI structural journal. 1998 Mar 1;95:107-15.

[2]. Khalifa A, Gold WJ, Nanni A, MI AA. Contribution of externally bonded FRP to shear capacity of RC flexural members. Journal of composites for construction. 1998 Nov;2(4):195-202.

[3]. Bousselham A, Chaallal O. Behavior of reinforced concrete T-beams strengthened in shear with carbon fiber-reinforced polymer-an experimental study. ACI structural Journal. 2006 May 1;103(3):339.

[4]. Chen JF, Teng JG. Shear capacity of fiber-reinforced polymer-strengthened reinforced concrete beams: Fiber reinforced polymer rupture. Journal of Structural Engineering. 2003 May;129(5):615-25.

[5]. Chen JF, Teng JG. Shear capacity of FRP-strengthened RC beams: FRP debonding. Construction and Building Materials. 2003 Feb 1;17(1):27-41.

[6]. Galal K, Mofidi A. Shear strengthening of RC T-beams using mechanically anchored unbonded dry carbon fiber sheets. Journal of Performance of Constructed Facilities. 2010 Feb;24(1):31-9.

[7]. Mofidi A, Thivierge S, Chaallal O, Shao Y. Behavior of reinforced concrete beams strengthened in shear using L-shaped CFRP plates: Experimental investigation. Journal of composites for construction. 2014 Apr 1;18(2):04013033.

[8]. Koutas L, Triantafillou TC. Use of anchors in shear strengthening of reinforced concrete T-beams with FRP. Journal of Composites for Construction. 2013 Feb 1;17(1):101-7.

[9]. El-Saikaly G, Godat A, Chaallal O. New anchorage technique for FRP shear-strengthened RC T-beams using CFRP rope. Journal of composites for construction. 2015 Aug 1;19(4):04014064.

[10]. Wahrhaftig AD, Rodrigues RB, Carvalho RF, Fortes AS. Strengthening reinforced concrete beams with carbon fiber laminate mounted in a u-shape for static and vibration purposes. International Journal of Civil Engineering. 2022 Jan;20:27-40.

[11]. Altun F. An experimental study of the jacketed reinforced-concrete beams under bending. Construction and Building Materials. 2004 Oct 1;18(8):611-8.

[12]. Martinola G, Meda A, Plizzari GA, Rinaldi Z. Strengthening and repair of RC beams with fiber reinforced concrete. Cement and concrete composites. 2010 Oct 1;32(9):731-9.

[13]. Souza RH, Appleton J. Flexural behaviour of strengthened reinforced concrete beams. Materials and Structures. 1997 Apr;30:154-9.

[14]. Diab YG. Strengthening of RC beams by using sprayed concrete: experimental approach. Engineering structures. 1998 Jul 1;20(7):631-43.

[15]. Ojaimi MF. Experimental Study on Shear Strengthening of Reinforced Concrete Beams Using Different Techniques of Concrete Jacketing. Basrah Journal for Engineering Science. 2021;21(2).

[16]. Tena-Colunga A, Hernandez-Marquez O, Archundia-Aranda HI. Strengthening of reinforced concrete prismatic and haunched beams using light jacketing. Journal of Building Engineering. 2020 Nov 1;32:101757.

[17]. Kamal A, Kunieda M, Ueda N, Nakamura H. Evaluation of crack opening performance of a repair material with strain hardening behavior. Cement and Concrete Composites. 2008 Nov 1;30(10):863-71.

[18]. Li VC, Horikoshi T, Ogawa A, Torigoe S, Saito T. Micromechanics-based durability study of polyvinyl alcohol-engineered cementitious composite. Materials Journal. 2004 May 1;101(3):242-8.

[19]. Kunieda M, Rokugo K. Recent progress on HPFRCC in Japan required performance and applications. Journal of Advanced Concrete Technology. 2006;4(1):19-33.

[20]. Hussein M, Kunieda M, Nakamura H. Strength and ductility of RC beams strengthened with steel-reinforced strain hardening cementitious composites. Cement and Concrete Composites. 2012 Oct 1;34(9):1061-6.

[21]. Li H, Xu S, Leung CK. Tensile and flexural properties of ultra high toughness cemontious composite. Journal of Wuhan University of Technology-Mater. Sci. Ed.. 2009 Aug;24(4):677-83.

[22]. Afefy HM, Mahmoud MH. Structural performance of RC slabs provided by pre-cast ECC strips in tension cover zone. Construction and Building Materials. 2014 Aug 29;65:103-13.

[23]. Afefy HM, Kassem NM, Mahmoud MH, Taher SE. Efficient strengthening of opened-joint for reinforced concrete broken slabs. Composite Structures. 2016 Feb 1;136:602-15.

[24]. Khalil AE, Etman E, Atta A, Essam M. Behavior of RC beams strengthened with strain hardening cementitious composites (SHCC) subjected to monotonic and repeated loads. Engineering Structures. 2017 Jun 1;140:151-63.

[25]. Ge WJ, Ashour AF, Ji X, Cai C, Cao DF. Flexural behavior of ECC-concrete composite beams reinforced with steel bars. Construction and Building Materials. 2018 Jan 20;159:175-88.

[26]. Zheng Y, Zhang LF, Xia LP. Investigation of the behaviour of flexible and ductile ECC link slab reinforced with FRP. Construction and Building Materials. 2018 Mar 30;166:694-711.

[27]. Bai L, Yu J, Zhang M, Zhou T. Experimental study on the bond behavior between H-shaped steel and engineered cementitious composites. Construction and Building Materials. 2019 Jan 30;196:214-32.

[28]. Ge W, Ashour AF, Cao D, Lu W, Gao P, Yu J, Ji X, Cai C. Experimental study on flexural behavior of ECC-concrete composite beams reinforced with FRP bars. Composite Structures. 2019 Jan 15;208:454-65.

[29]. Ding Z, Fu J, Li X, Ji X. Mechanical behavior and its influencing factors on engineered cementitious composite linings. Advances in Materials Science and Engineering. 2019 Aug 14;2019.

[30]. Wang N. Experimental research on bonding mechanical performance between ultra high toughness cementitious composites (UHTCC) and existing concrete. Dalian, China: Dalian University of Technology. 2011.

[31]. Slowik V, Luković M, Wagner C, van Zijl GP. Behaviour of bonded SHCC overlay systems. A Framework for Durability Design with Strain-Hardening Cement-Based Composites (SHCC) State-of-the-Art Report of the RILEM Technical Committee 240-FDS. 2017:125-46.

[32]. Kim YY, Fischer G, Lim YM, Li VC. Mechanical performance of sprayed engineered cementitious composite using wet-mix shotcreting process for repair applications. Materials Journal. 2004 Jan 1;101(1):42-9.

[33]. Kim SW, Park WS, Jang YI, Feo L, Yun HD. Crack damage mitigation and shear behavior of shear-dominant reinforced concrete beams repaired with strain-hardening cement-based composite. Composites Part B: Engineering. 2015 Sep 15;79:6-19.

[34]. Wang G, Yang C, Pan Y, Zhu F, Jin K, Li K, Nanni A. Shear behaviors of RC beams externally strengthened with engineered cementitious composite layers. Materials. 2019 Jul 5;12(13):2163.

[35]. Hassan A, Baraghith AT, Atta AM, El-Shafiey TF. Retrofitting of shear-damaged RC T-beams using U-shaped SHCC jacket. Engineering Structures. 2021 Oct 15;245:112892.

[36]. Baghi H, Barros JA, Rezazadeh M. Shear strengthening of damaged reinforced concrete beams with Hybrid Composite Plates. Composite Structures. 2017 Oct 15;178:353-71.

[37]. Afefy HM, Baraghith AT, Hassan A, Abuzaid MK. Strengthening of shear-deficient RC beams using near surface embedded precast cement-based composite plates (PCBCPs). Engineering Structures. 2021 Oct 1;244:112765.
[38]. Baraghith AT, Mansour W, Behiry RN, Fayed S. Effectiveness of SHCC strips reinforced with glass fiber textile mesh layers for shear strengthening of RC beams: Experimental and numerical assessments. Construction and Building Materials. 2022 Apr 11;327:127036.
[39]. Baraghith AT, Khalil AH, Etman EE, Behiry RN. Improving the shear behavior of RC dapped-end beams using precast strain-hardening cementitious composite (P-SHCC) plates. InStructures 2023 Apr 1 (Vol. 50, pp. 978-997).
[40]. Khalil AE, Atta AM, Baraghith AT, Behiry RN, Soliman OE. Shear strengthening of concrete deep beams using pre-fabricated strain-hardening cementitious composite plates. Engineering Structures. 2023 Mar 1;278:115548.
[41]. ASTM C39/C39M-21. Standard Test Method for Compressive Strength of Cylindrical Concrete Specimens. ASTM International, 2021.
[42]. Afefy HM, Baraghith AT, Hassan A, Abuzaid MK. Strengthening of shear-deficient RC beams using near surface embedded precast cement-based composite plates (PCBCPs). Engineering Structures. 2021 Oct 1;244:112765.
[43]. ASTM A615/A615M-16. Standard specification for deformed and plain carbon steel bars for concrete reinforcement. ASTM International, 2016.
[44]. ACI Committee. Building code requirements for structural concrete (ACI 318-19) and commentary. American Concrete Institute, Farmington Hills, MI, 519 ppfv, 2019.
[45]. Khalil AE, Etman E, Atta A, Baraghith A, Behiry R. The effective width in shear design of wide-shallow beams: a comparative study. KSCE Journal of Civil Engineering. 2019 Apr;23:1670-81.
[46]. Li B, Lam ES, Wu B, Wang YY. Experimental investigation on reinforced concrete interior beam–column joints rehabilitated by ferrocement jackets. Engineering Structures. 2013 Nov 1;56:897-909.
[47]. Afefy HM, Baraghith AT, Mahmoud MH. Retrofitting of defected reinforced-concrete cantilever slabs using different techniques. Magazine of Concrete Research. 2020 Jul;72(14):703-19.
[48]. Alyousif A, Anil O, Sahmaran M, Lachemi M, Yildirim G, Ashour AF. Comparison of shear behaviour of engineered cementitious composite and normal concrete beams with different shear span lengths. Magazine of Concrete Research. 2016 Mar;68(5):217-28.

Reda N. Behiry, et. al. "Strain-Hardening Cementitious Composites Versus Normal Mortar for Shear Strengthening of Concrete Beams." *IOSR Journal of Mechanical and Civil Engineering (IOSR-JMCE),* 20(2), 2023, pp. 61-75.